Catalysis Letters Vol. 103, Nos. 3–4, October 2005 (© 2005)
DOI: 10.1007/s10562-005-7159-1

The effect of the addition of Re and Ge on the properties of Pt/Al_2O_3

M.C. Souza Santos[a], J.M. Grau[a], C.L. Pieck[a], J.M. Parera[a], J.L.G. Fierro[b], N.S. Fígoli[a,*], and M.C. Rangel[c]

[a]*INCAPE, Instituto de Investigaciones en Catálisis y Petroquímica (FIQ-UNL, CONICET), Santiago del Estero 2654, 3000 Santa Fe, Argentina*
[b]*CSIC, Instituto de Catálisis y Petroleoquímica, Campus UAM, Cantoblanco, 28049 Madrid, Spain*
[c]*GECCAT Grupo de Estudos em Cinética e Catálise, Universidade Federal da Bahia, Campus Universitário de Ondina, Federação, 41170280 Salvador, Bahia, Brazil*

Received 6 June 2005; accepted 6 August 2005

The effect of Re and Ge addition to Pt/Al_2O_3 was studied. Mono-, bi- and a trimetallic catalysts were prepared and characterized by TPR, XPS, TPO and by the *n*-pentane, cyclohexane (CH) and *n*-octane reactions. It was found that the trimetallic was the most active and stable catalyst and showed selectivities to aromatics and isomers very similar to the bimetallic germanium-based catalyst.

KEY WORDS: naphtha reforming; trimetallic catalysts; Pt–Re–Ge.

1. Introduction

Catalytic naphtha reforming is one of the most important refining and petrochemical processes, in which naphtenes and paraffins are transformed into isomeric and aromatic hydrocarbons [1–4]. Hydrogen is an important by-product [2]. The catalyst is bifunctional, being Pt/Al_2O_3 the first to be used; it was then replaced by the so-called bimetallic [5,6], trimetallic and multimetallic catalysts. There is not much information regarding whether the addition of a new element affects only the metallic function or if it also affects the acid function. The most studied, among bimetallic catalysts, is $Pt–Re/Al_2O_3$ [7–11]. Regarding the trimetallic catalysts, there is not much information in the open literature about their properties. There have been recently published studies about the effect of Re and Sn addition to Pt/Al_2O_3 on its acid and metallic functions [12,13]. These studies showed that Re and Sn affect not only the metallic but also the acid function. The modifications are different according to the order of the metals addition. One interesting catalyst could be $Pt–Re–Ge/Al_2O_3$; this system was patented [14] but not studied in the open literature.

The objective of this paper is to study the influence of the addition of Re and Ge to a Pt/Al_2O_3 catalyst.

2. Experimental

2.1. Catalysts preparation

Catalysts were prepared using γ-Al_2O_3 Ketjen CK-300 ($S_g = 180\ m^2g^{-1}$, $V_g = 0.49\ cm^3g^{-1}$) as support. The pellets were crushed up to 35–80 mesh and calcined at 650 °C under an air stream (100 mL min^{-1}). The following catalysts were prepared by wet impregnation: Pt, Pt–Re, Pt–Ge and Pt–Re–Ge. The metal precursors were H_2PtCl_6, NH_4ReO_4 and $GeCl_4$ in appropriate concentrations such as to obtain about 0.3% of each element in the final catalyst. In the case of the bi- and the trimetallic catalysts, the addition of the precursors was carried out by co-impregnation. The impregnates were dried at 120 °C and calcined at 500 °C for 3 h and finally reduced at the same temperature for 3 h under a hydrogen stream.

2.2. Catalyst characterization

The Pt, Re- and Ge-content of the solids was determined by atomic emission spectroscopy (ICP-AES) using a ARL model 3410 equipment. The solids were dissolved in a digestive pump with a mixture of 1 mL sulphuric acid, 3 mL hydrochloric acid and 1 mL nitric acid. The chlorine content of the catalysts was determined by the Volhard–Charpenter method.

Thermal programmed reduction (TPR) tests were performed in an Ohkura TP2002 equipment provided with a thermal conductivity detector. At the beginning of each test the catalyst samples were pre-treated *in situ* heating in air at 450 °C for 1 h. Temperature was decreased and then the samples were heated from room temperature to 750 °C at 10 °C min^{-1} in a gas stream of 5% hydrogen in argon.

X-ray Photoelectron Spectra (XPS) were recorded with a VG Escalab 200R electron spectrometer equipped with a hemispherical electron analyzer, using an MgKα ($h\nu = 1253.6$ eV) X-ray source. An ECLIPSE software package was used for acquisition and data analysis. Peak intensities were estimated by calculating the integral of each peak after subtraction of an S-shaped

* To whom correspondence should be addressed.
E-mail: nfigoli@fiqus.unl.edu.ar

1011-372X/05/1000–0229/0 © 2005 Springer Science+Business Media, Inc.

background and fitting the experimental curve to a combination of Gaussian and Lorentzian lines. The C1s peak (contamination) at a binding energy (BE) of 284.9 eV was taken as an internal standard for BE measurements. Surface atomic ratios were determined from the intensity ratios normalized by atomic sensitivity factors [15].

FTIR spectra of pre-reduced and evacuated samples were taken at room temperature in a Nicolet 5ZDX spectrometer in the 400–4800 cm^{-1} range with a resolution of 4 cm^{-1}. Self supported wafers were successively reduced at 400 °C under hydrogen flow for 30 min and outgassed at 10^{-6} Torr at 500 °C for 30 min. After recording the IR spectrum, the samples were contacted with 30 Torr of CO for 5 min and then a second spectrum was recorded. Then the sample was outgassed at 10^{-6} Torr at room temperature for 30 min and a new spectrum was obtained. The absorbance of chemisorbed CO without evacuation and outgassed at room temperature, were obtained by subtracting the first spectrum of the respective spectra.

The reaction of dehydrogenation of cyclohexane (CH) to benzene was used as test reaction of the metal function and its poisoning by sulphur. The CH was Merck for spectroscopy, 99.9% pure; the provider states a sulphur upper limit of 0.001%, but to assure a very low sulphur level, the liquid CH was kept over Pt/Al_2O_3, that adsorbs the sulphur. The reaction was carried out at atmospheric pressure, 400 °C, WHSV = 10 and H_2:CH(molar) = 30. The analysis of reactants and products was performed on line using a Varian 3400 CX gas chromatograph equipped with a FID and a packed column of FFAP on Chromosorb (ID 1/8″ in, 3 m length) maintained at 64 °C was used for products separation. The test started feeding pure CH during 1 h. After, the CH feed was doped with 5 ppm S as CS_2 and the run continued during another hour. The CH feed was stopped and pure hydrogen was allowed to flow for 4 h at 400 °C in order to remove reversibly adsorbed sulphur. Then, a last step was performed: pure CH was passed again and the reaction conditions were set as those of the beginning, to see the recovering of the catalytic activity and the degree of irreversible poisoning.

The reaction test of *n*-pentane (*n*-C_5), for the acid function, was carried out for 4 h in a continuous flow glass reactor at atmospheric pressure, 500 °C, WHSV = 4.5 and molar ratio H_2: *n*-C_5 = 6. *n*-C_5 was supplied by Merck (99.9%). Analysis of reactants and products were performed by on-line GC with a packed column of dimethyl sulfolane on Chromosorb P (ID 1/8" in, 3 m length) maintained at 40 °C.

The reforming of *n*-octane (*n*-C_8) was used as test reaction of the two functions. The *n*-octane was Carlo Erba RPE, 99% pure (GLC) and the hydrogen was pure, provided by AGA. The reaction was performed at atmospheric pressure, 450 °C, WHSV = 3.4 and H_2/nC_8 (molar) = 7.3. The time-of-stream (TOS) was 6 h. The reaction products were analysed by on-line gas chromatography in a Shimadzu GC-8A chromatograph equipped with a 100 m capillary column of cupper coated with squalene and a FID. From these data, *n*-octane conversion and yields to the different reaction products (on a carbon basis) were calculated. The selectivity to *i* species is defined as ($10^2\times$ yield of *i*/total conversion).

Under the reaction conditions chosen for the three reactions, neither internal nor external mass transfer limitations in the catalyst particles were found, as confirmed by the calculation of the Weisz–Prater modulus ($Z < 0.01$) and the Damköhler number ($Da \asymp 0$), respectively. For these calculations, kinetic parameters were conservatively estimated from maximum initial reaction rate values by assuming first-order kinetics and transport coefficients were estimated from known correlations.

The coke deposited on the catalysts at the end of the *n*-C_8 reaction was analysed by temperature programmed oxidation (TPO). 30–50 mg of a coked catalyst were placed in a quartz cell. Then the carbon deposits were continuously oxidized with a stream of 5% O_2:N_2 (vol/vol) flowing at 40 mL min^{-1}. The cell was heated from room temperature to 650 °C using a heating rate of 10 °C min^{-1}. The gases issuing from the cell were fed to a methanation reactor where CO_2 and CO were quantitatively transformed into CH_4 over a Ni catalyst and in the presence of H_2. The methanator outlet was directly connected to a FID detector and the signal was continuously sampled and recorded. The carbon concentration on the catalysts was calculated from the area of the TPO diagram area by careful calibration with TPO of standard samples of known carbon content.

3. Results and discussion

The composition of the catalysts is presented in table 1. Pt and Re content is about 0.3%, while the Ge content is about 0.2%. They have about 0.9% Cl which is a typical value for commercial naphtha reforming catalysts [4].

The TPR profiles are presented in figure 1. Pt/Al_2O_3 presents a peak at 225 °C, attributed to the reduction of oxychloride platinum species and a small one at 350 °C associated with the reduction of species in strong interaction with the support [16]. Re/Al_2O_3 and Ge/Al_2O_3 samples show a peak at about 600 °C corresponding to the reduction of the respective oxides [10,17]. Pt–Re/Al_2O_3 presents two peaks at 225 and 580 °C, respectively; the first is attributed to the reduction of platinum and rhenium oxides placed near platinum and the second to segregated rhenium in strong interaction with the support [10]. This second peak is at 20 °C less than in Re/Al_2O_3, indicating that there is a catalytic action of Pt

Table 1
Composition of the catalysts

Catalyst	wt %			
	Pt	Re	Ge	Cl
Pt/Al_2O_3	0.30	–	–	0.94
$Pt–Re/Al_2O_3$	0.30	0.32	–	0.84
$Pt–Ge/Al_2O_3$	0.29	–	0.22	0.92
$Pt–Re–Ge/Al_2O_3$	0.29	0.30	0.21	0.87

on Re oxide reduction. $Pt–Ge/Al_2O_3$ presents three peaks at 280, 400 and 630 °C. If a comparison is made between this profile and that of Pt/Al_2O_3 it can be seen that the two first peaks were shifted to higher temperatures. It can not be neglected the possibility of Pt–Ge alloying. Previous works using Pt–Ge/ Al_2O_3 samples reduced at 650 °C [17–20] showed that germanium is present as Ge^{2+} and Ge^0, the last one being alloyed with Pt. The shift to higher temperatures in the two Pt oxide reduction peaks observed in $Pt–Ge/Al_2O_3$ is indicative that Ge retards Pt oxide reduction due to interaction or coverage of Pt by Ge and that Pt catalyses the reduction of Ge oxide [18]. The last peak is shifted to higher temperatures, when comparing to Ge/Al_2O_3. This result indicates that part of the Ge oxide particles were segregated, interacting with the support. Some differences with the literature cited above can be explained considering differences in metal precursors and preparation methods that influence the metallic clusters [21]. $Pt–Re–Ge/Al_2O_3$ presents two peaks: the first at 280 and the second at 600 °C. Comparing with the monometallic and bimetallics catalysts, the first peak can be assigned to the reduction of platinum oxide and to the co-reduction of oxides of the other elements placed around Pt. The other peak can be assigned to the reduction of segregated rhenium and germanium oxides in interaction with the support because they have the same temperature that the last peak in Re/Al_2O_3 and Ge/Al_2O_3.

Table 2 presents the XPS results and figure 2 displays the Pt $4d_{5/2}$ line profiles of samples reduced *in situ* at 500 °C. The BEs of the Pt $4d_{5/2}$ and Ge $2p_{3/2}$ peaks, as well as the Pt/Al and Ge/Al atomic ratios are presented. The presence of Re was not detected following the Re $4f_{7/2}$ signal, indicating that Re is not exposed on the external surface of catalyst particles, it is deposited inside the pores. This is due to the competitive adsorption on the support sites, during the catalyst preparation, between the $[Cl_6Pt]^{2-}$ and $[ReO_4]^-$ complex anions. The higher the charge of the anion, the higher the electrostatic attraction with the adsorption sites [22]. Then, $[Cl_6Pt]^{2-}$ is adsorbed first and stronger than $[ReO_4]^-$ and this anion must migrate to free adsorption sites in the particle inner part. This was shown [23] experimentally and by modelling the diffusion–adsorption phenomena of both anions; in all cases Re was

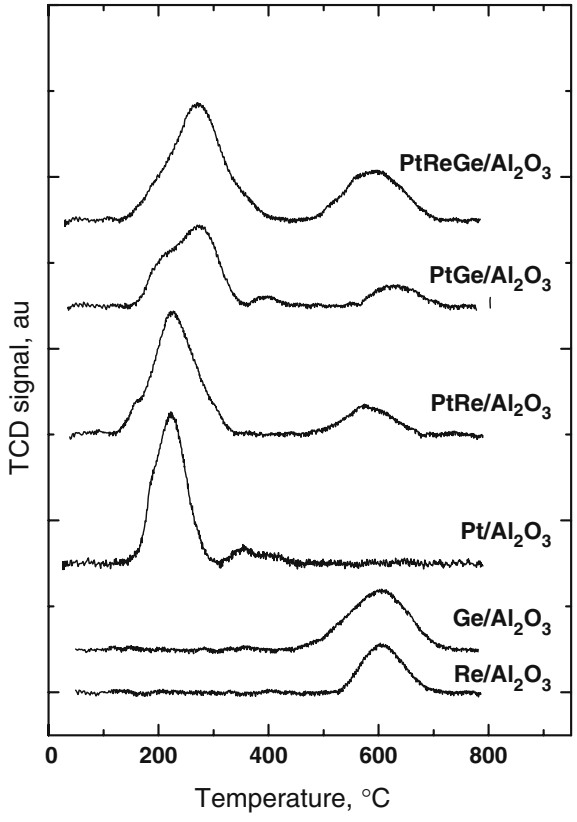

Figure 1. TPR profiles of the catalysts.

Table 2
Binding energies (eV) of core electrons of alumina supported catalysts and surface atomic ratio Pt/Al and Ge/Al

Catalyst	Pt $4d_{5/2}$	Ge $2p_{3/2}$	$Pt/Al \times 10^3$ (at/at)	$Ge/Al \times 10^3$ (at/at)
Pt/Al_2O_3	314.9	–	0.53	–
$Pt–Re/Al_2O_3$	314.8	–	0.46	–
$Pt–Ge/Al_2O_3$	315.3	1220	0.43	1.02
$Pt–Re–Ge/Al_2O_3$	315.3	1220	0.44	

The Al 2p binding energy is 74.5 eV for all catalysts.

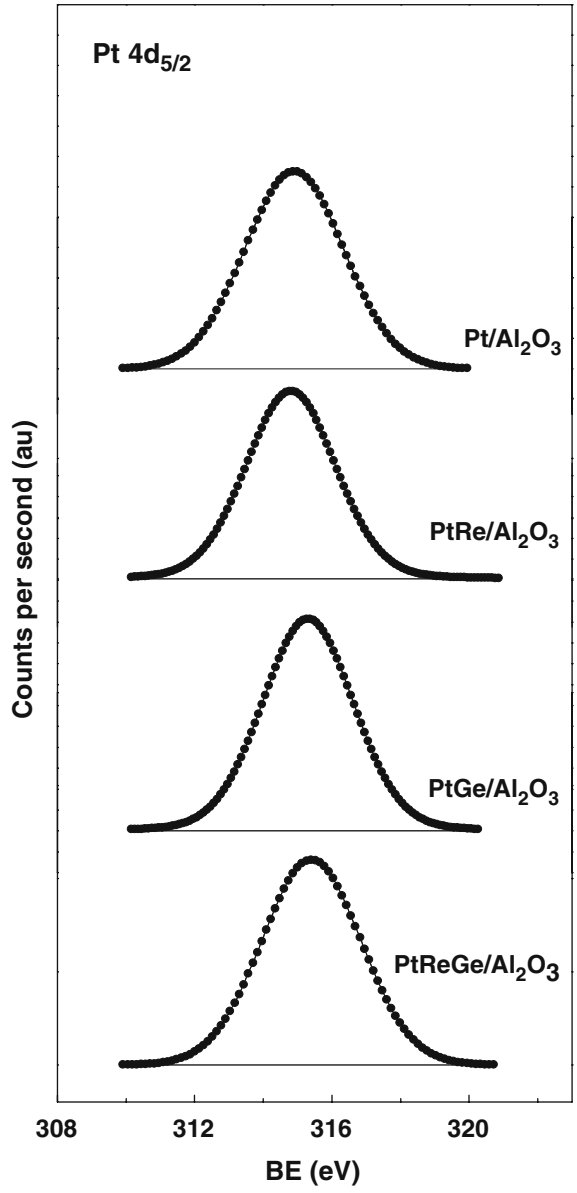

Figure 2. Pt $4d_{5/2}$ line profiles of catalysts pre-reduced under H_2 at 500 °C for 1 h.

more concentrated inside the pores. The Al 2p signal appears at 74.5 eV for all catalysts, meaning that the electronic state of aluminium is not affected by the supported metals. In the Pt $4d_{5/2}$ line profiles the full width at half maximum values, higher than 2.0 eV in all cases, suggests the possible presence of more than one platinum species. The presence of Ge affects more the electronic state of Pt than Re. Platinum is more electrodeficient in Pt–Ge than in the monometallic Pt. The Pt/Al atomic ratio decreases when either Re or/and Ge are present. Possible explanations to this decrease could be: (a) different Pt distribution inside the catalyst particles, (b) the other elements may be covering the Pt sites or (c) Re and/or Ge may favour the production of bigger crystallites of platinum. Considering case (a), during the preparation of the monometallic Pt catalyst the only adsorbed anion is $[Cl_6Pt]^{2-}$ which, as quoted above, has a great affinity for the support adsorption sites, thus producing a great adsorption on the support external surface and on the pore mouths, and low migration and adsorption inside the pores. Regarding bi- and trimetallic catalysts, the competition for adsorption produces a greater migration of $[Cl_6Pt]^{2-}$ inside the pores [23]. The different distribution of Pt produces a lower Pt/Al ratio by XPS because this technique only shows the ratio at the outermost surface of the catalyst. Considering (b), Pt coverage by Re cannot exist because Re is not present in the particle zone seen by XPS. Case (c) can be discarded because it does not agree with accepted literature. Since the early studies on Pt–Re catalysts, it was stated that Re produces stabilization of the Pt crystals on the support [22]. For Pt–Ge, it was shown [19] that the addition of Ge practically does not affect the Pt dispersion. Using Transmition Electron Microscopy it was shown [12] that the mean particle size of Pt crystals in monometallic Pt was 1.8, 1.5 nm in Pt–Re, 1.8 nm in Pt–Sn and 1.9–2.0 nm in Pt–Re–Sn. The behaviour of Sn in these catalysts is quite similar to the one of Ge. Then, the addition of Re and Ge does not produce bigger Pt crystallites. We can conclude that the different Pt profiles in the catalysts and the limited extension of XPS analysis is the reason of the decrease in the Pt/Al ratio.

FTIR spectra of CO chemisorbed was used to study the nature of the metal surface sites in reduced catalysts. CO is adsorbed in the linear and bridging forms on Pt particles, and the wavenumber zone corresponding to the linear CO reports the most relevant information to study the electronic change in the metal surface. The parameters of the spectra (position of maximum of peaks and shoulders and area percentage of each band) obtained with the different samples, Pt, Pt–Re, Pt–Ge, and Pt–Re–Ge catalysts, are shown in table 3. The infrared spectrum of CO adsorbed on the Pt catalyst displays a well resolved absorption band at 2075 cm^{-1}, corresponding to linearly adsorbed CO on metallic platinum (Pt^0–CO) [24]. In contrast to the Pt catalyst, Re and Ge samples do not show any absorption band. Hence, the absorption bands observed in the bimetallic and trimetallic samples can be attributed to platinum species modified by the promoters. As shown in table 3,

the adsorption of CO over Pt–Re catalyst shows a spectra that presents the main band of Pt–CO lightly shifted (relative to monometallic Pt) to 2072 cm^{-1} and a shoulder appears at 2011 cm^{-1}, that is assigned to Pt influenced by Re ($Pt^{\delta-}$–CO) [12], indicating electronic transfer from Re to Pt. On Pt–Ge, the absorption band maximum is shifted to a higher frequency: 2083 cm^{-1}. This upward shift can be explained by considering that Ge acts as an electron-acceptor [25], decreasing the electronic density of platinum. Moreover, a shoulder at 2120 cm^{-1} appears, that is assigned to CO bonded on $Pt^{\delta+}$ [26].

The spectrum of Pt–Re–Ge/Al_2O_3 and its deconvolution is shown in figure 3. An absorption band at 2079 (2), with shoulders at 2102 (1), 2011 (3) and 1978 cm^{-1} (4) can be noticed. The band at 2079 cm^{-1}, corresponds to Pt in low electronical interaction with Re and Ge. Comparing with the spectra of bimetallic catalysts, the shoulder at 2102 cm^{-1} corresponds to CO adsorbed on Pt influenced by Ge and the shoulder at 2011 cm^{-1} corresponds to CO adsorbed on Pt influenced by Re. The other band at a lower wavenumber, 1978 cm^{-1}, is not present on Pt–Ge neither on Pt–Re and could correspond to Pt affected simultaneously by Ge and Re. A similar spectrum was obtained with a trimetallic Pt–Re–Sn catalyst [12]. The presence of a peak at 1978 cm^{-1} in Pt–Re–Ge means an electronic transfer from the other elements to Pt.

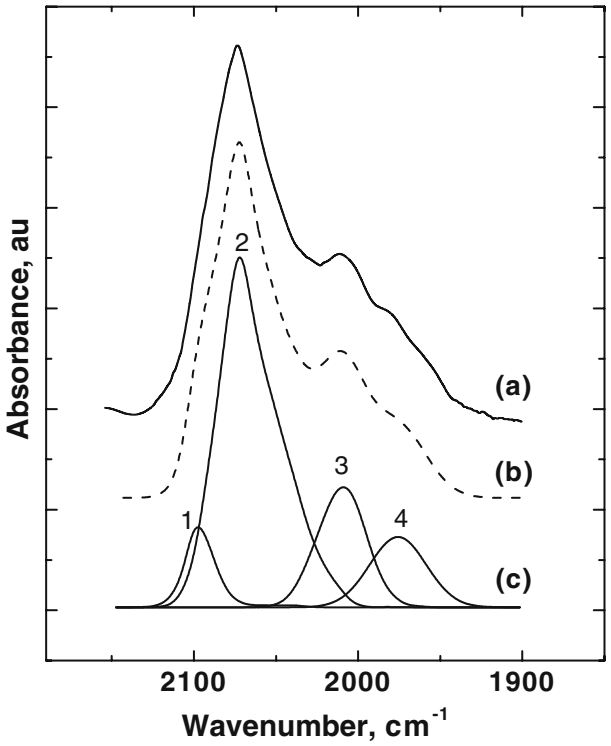

Figure 3. FTIR spectrum of CO linearly adsorbed at 20 °C on Pt–Re–Ge/Al_2O_3. (a) Experimental spectrum; (b) sum of deconvoluted peaks; (c) peaks obtained after deconvolution.

Figure 4 shows the activity and sensitivity to sulphur of the catalysts during the CH reaction. At the operational conditions used, this reaction is selective to benzene and stable during the 60 min TOS. The highest conversion is obtained with Pt/Al_2O_3, followed by Pt–Re, Pt–Ge and Pt–Re–Ge. As found by other authors [17,18,27], the addition of either Re or Ge decreases the dehydrogenating activity of Pt. It can be noted that the effect is more pronounced when both elements are present, similarly to the case of the electronic transfer shown by IR spectroscopy. The decrease in activity upon the addition of the other elements can be ascribed to an electronic effect on Pt, perhaps induced by metals atoms placed in the neighbourhood and by stoichiometric alloys formation. These alloys are inactive for the hydrogenation reaction, [28] and the less interacted Pt atoms present a lower catalytic activity than the one of neutral Pt^0. According to [12] the maximum in catalytic activity corresponds to Pt^0 and the activity decreases when Pt is not neutral, $Pt^{\delta+}$ or $Pt^{\delta-}$. Ge decreases the Pt CH dehydrogenation capacity in a greater extent than Re, in agreement with the greater Pt electronic modification shown by XPS.

After 1 h TOS, the pure CH feed was changed for the one containing S and a deactivation of the catalysts was observed. At the operational conditions used, after 30 min, the sulphur coverage of Pt/Al_2O_3 is in adsorption equilibrium with the sulphur of the reactant stream and the conversion reaches a constant value. Pt–Re/Al_2O_3 needs 45 min because S is adsorbed on Pt and Re

Table 3
Position of the maximum of the peaks obtained by deconvolution of the experimental spectrum of CO linearly absorbed on Pt having different superficial electronic densities

Catalyst	ν_{CO}, cm^{-1}/Area, %			
	$GePt^{\delta+}$	Pt	$RePt^{\delta-}$	$GRePt^{\delta-}$
Pt/Al_2O_3	–	2075/100	–	–
Pt–Re/Al_2O_3	–	2072 / 81	2011 / 19	–
Pt–Ge/Al_2O_3	2120 / 13	2083 / 87	–	–
Pt–Re–Ge/Al_2O_3	2102 / 11	2079 / 58	2011 / 18	1978 / 13

The spectrum was taken after CO adsorption and evacuation at 10^{-6} Torr and 25 °C during 30 min. Area percentage values of the bands are also given.

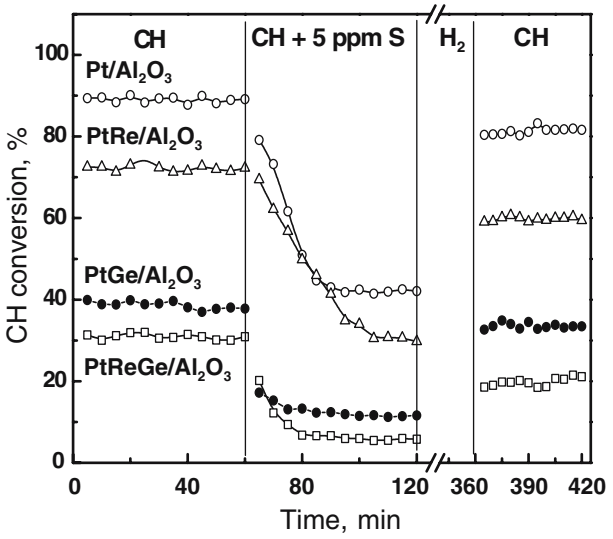

Figure 4. Cyclohexane conversion as a function of time. Reaction conditions: 400 °C, 0.1 MPa, H_2/nC_8 (molar) = 30, WHSV = 10.

surfaces. The time required to reach equilibrium on Pt–Ge/Al_2O_3 and Pt–Re–Ge/Al_2O_3 is smaller because of the smaller number of Pt active sites (Pt is partially alloyed). After 4 h of reversible S elimination with hydrogen, the catalytic activity is partly recovered. The recovering depends on the strength of the Pt–S bond. The weaker this bond, the higher the fraction of S desorbed and the greater the fraction of the original catalytic activity that is recovered. For Pt/Al_2O_3 the recovering of the catalytic activity is 90% of the initial one, for Pt–Re/Al_2O_3 is 81%, for Pt–Ge/Al_2O_3 the value is 91% and for Pt–Re–Ge/Al_2O_3, 60%. These results show that the Pt–S bond is weaker on Pt–Ge/Al_2O_3 than on Pt–Re/Al_2O_3 and that the trimetallic catalyst is very sensitive to the sulphur poisoning.

Figure 5 presents the *n*-pentane conversion values as a function of time. Pt–Re–Ge/Al_2O_3 and Pt–Ge/Al_2O_3 are the most active catalysts for the reaction, having the last one the highest initial activity, but conversion decreases as a function of time. The most stable catalyst is the trimetallic one. These results show that both rhenium and germanium have favourable effects on Pt for this reaction and that the presence of both Ge and Re leads to very stable active sites.

The main product of the *n*-pentane reaction is *i*-pentane, while C_1–C_4 products are also produced. The isomerization mechanism over platinum supported catalysts is considered as a bifunctional metal-acid one [29], being controlled by the acid function [30]. Therefore, the *i*-pentane, as well as C_3 formation can be taken as a measure of the acid function. C_1, a hydrogenolysis product, can be taken as a measure of the metal function. Table 4 presents the selectivity to *i*-pentane (S_{iC5}), the molar ratio C_3/C_1 and the selectivity to C_1 (S_{C1}) at two times on stream. The highest metallic activity (selectivity to C_1) is presented by Pt/Al_2O_3 in accordance with the

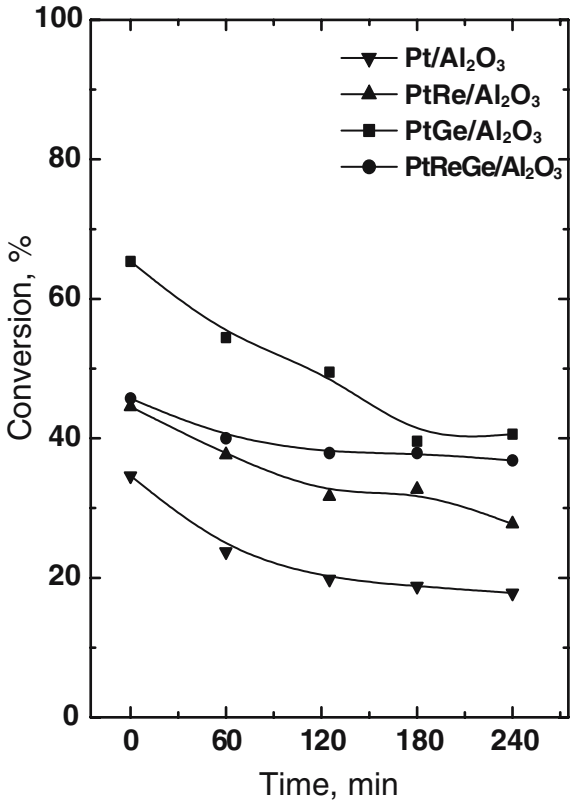

Figure 5. *n*-Pentane conversion as a function of time. Reaction conditions: 400 °C, 0.1 MPa, H_2/nC_8 (molar) = 30, WHSV = 10.

results of the CH reaction. Pt/Al_2O_3 shows the highest decrease in metallic activity with TOS. It can be noted that the presence of Ge decreases the hydrogenolysis function of the catalysts, which is very small after 240 min of reaction. It can be also noted that both Ge and Re affect the acid function, being the strongest effect showed by Ge. In fact, the Ge-based catalysts showed the highest selectivity to *i*-pentane. In addition, the trimetallic catalyst is able to keep this value very close to the initial one, showing that the acid function is resistant against deactivation under the operational conditions. The C_3/C_1 molar ratio indicates the balance of the metal and acidic functions. From table 4, one can see that both metals increase this ratio due to a decrease in hydrogenolysis to C_1. Germanium is able to decrease the hydrogenolysis at the end of the reaction, meaning that it can increase the selectivity to heavier products. This explains why the selectivity to *i*-pentane is kept in high values at the end of the reaction. This effect seems to be stronger in the trimetallic catalyst which showed an increase in selectivity towards *i*-pentane during the reaction.

Figure 6 shows the modifications of conversion during the *n*-octane reaction as a function of time. At 5 min TOS the conversion is very similar for the four catalysts, although Re enhances and Ge decreases slightly the activity of Pt/Al_2O_3. The bimetallics and the trimetallic catalyst are stabilized at about 300 min TOS, while Pt/Al_2O_3 is still decreasing its activity at that time. The

Table 4
C_3/C_1 molar ratio and selectivity to C_1 (S_{C1}) and to *i*-C_5 (Si_{C5}) at two TOS during the *n*-pentane reaction

Catalyst	Time (min)	C_3/C_1 (molar)	S_{C1}(%)	Si_{C5} (%)
Pt/Al_2O_3	5	1.4	1.9	36.0
	240	2.9	0.5	22.4
$Pt–Re/Al_2O_3$	5	2.8	0.7	42.0
	240	2.4	0.7	33.2
$Pt–Ge/Al_2O_3$	5	2.8	0.7	58.2
	240	5.8	0.2	49.4
$Pt–Re–Ge/Al_2O_3$	5	6.2	0.2	41.6
	240	4.0	0.3	48.9

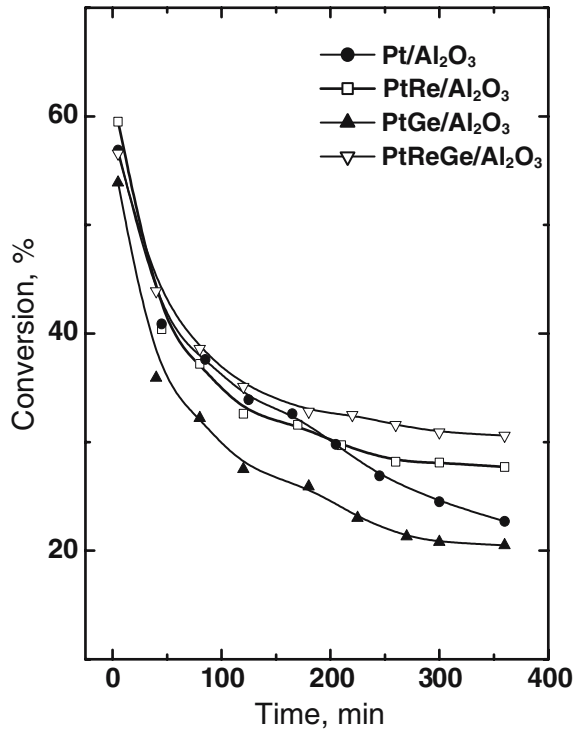

Figure 6. *n*-Octane conversion as a function of time. Reaction conditions: 450 °C, 0.1 MPa, H_2/nC_8 (molar) = 7.3, WHSV = 3.4.

highest activity at 300 min TOS is obtained with the trimetallic catalyst.

At 5 min TOS, the conversion values are very similar, and the modifications of selectivity produced by the introduction of other elements to Pt/Al_2O_3 can be analysed. The selectivity values are presented in table 5 and the yield to aromatic products are represented in figure 7. The addition of Re to Pt increases the selectivity to total aromatics (from 47.1% to 53.4%) and decreases the isomerization (from 34.6% to 31.4%). The addition of Ge reduces the total aromatics (from 47.1% to 45.4%) and increases the isomerization (from 34.6% to 42.2%). A similar effect of Ge over Pt was found by Galisteo et al. [25]. $Pt–Re–Ge/Al_2O_3$ has almost the same selectivity than $Pt–Ge/Al_2O_3$ but is more stable(selectivity to total aromatics, 46.7% and selectivity to isomers, 41.1%).

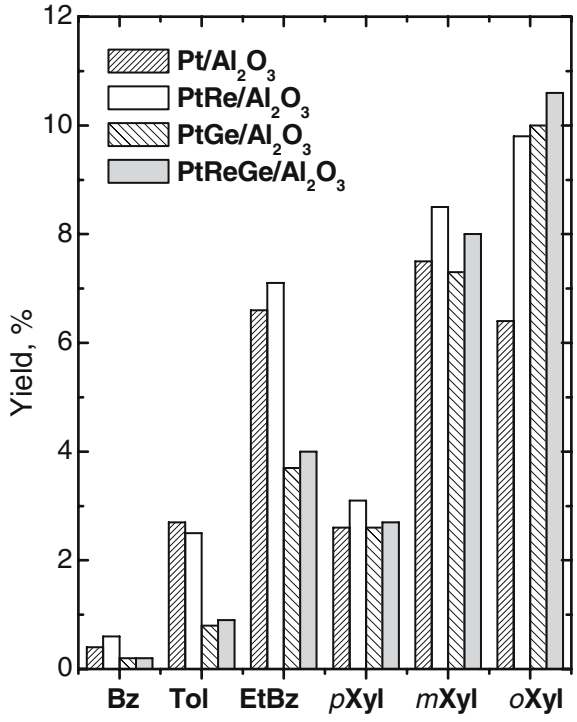

Figure 7. Yield to each aromatic for monometallic, bimetallic and trimetallic catalyst during the *n*-octane reaction at 5 min TOS. Reaction conditions: 450 °C, 0.1 MPa, H_2/nC_8 (molar) = 7.3, WHSV = 3.4.

Then, the influence of Re and Ge on Pt have opposite effects regarding the isomers/aromatics selectivities ratio. In the trimetallic the influence of Ge is more important than the one of Re. The ratio is important in reformulated gasolines where the content of aromatic hydrocarbons must be decreased and the corresponding loss of octane number can be partially recovered increasing the isomers concentration. The ratio values at 5 min TOS for the tested catalysts are: Pt/Al_2O_3, 0.73; $Pt–Re/Al_2O_3$, 0.59; $Pt–Ge/Al_2O_3$, 0.93; and $Pt–Re–Ge/Al_2O_3$, 0.88. Table 5 also shows that Pt/Al_2O_3 and $Pt–Re/Al_2O_3$ present higher hydrogenolytic activities than the other catalysts, producing higher amounts of C_1, C_2, benzene and toluene. In commercial practice, the hydrogenolytic activity is decreased by catalyst sulfidation and in the case of the catalysts with Ge, it produces a similar effect than sulfidation. During the run the production of light isomers (C_4–C_7) decreases and the production of i-octanes increase. This isomers are intermediate products that are produced very rapidly and they are then hydrocracked to light isomers, reaction that is deactivated during the run.

Looking to the C_8 aromatics yields distribution shown in figure 7, it can be seen that Ge addition decreases the yield in ethylbenzene and highly increases the yield in *o*-xylene. It can be seen that the addition to Pt of Re or Ge or both of them, mainly increases the

Table 5
Total conversion (X) and selectivity to each product during the *n*-octane reforming at 5 and 360 min

Catalyst	Pt/Al_2O_3		$Pt–Re/Al_2O_3$		$Pt–Ge/Al_2O_3$		$Pt–Re–Ge/Al_2O_3$	
TOS (min)	5	360	5	360	5	360	5	360
X %	55.6	22.7	59.3	27.7	53.8	20.5	56.5	30.6
Selectivity to (%)								
C_1	0.8	0.4	0.4	0.3	0.2	0.1	0.2	0.2
C_2	1.6	1.4	1.5	1.2	1.0	0.6	1.1	1.0
C_3	2.9	3.2	2.6	2.4	2.4	2.0	2.3	1.9
iC_4	1.1	0.6	0.6	0.4	0.9	0.2	1.0	0.4
nC_4	3.1	3.8	2.7	2.6	2.5	2.2	2.4	2.0
iC_5	2.2	1.2	1.7	0.9	2.2	0.6	2.4	1.0
nC_5	2.5	2.8	2.2	2.2	2.0	1.8	2.0	1.7
$C_5^=$	0.8	2.4	0.4	1.8	0.7	1.7	0.6	1.0
iC_6	2.7	2.2	2.1	1.8	2.5	1.5	2.7	1.6
nC_6	2.0	2.8	1.7	2.4	1.7	2.1	1.7	1.7
MCP + CH	1.2	0.6	0.7	0.5	0.3	0.3	0.3	0.2
Bz	0.8	0.3	1.0	0.4	0.3	0.2	0.3	0.1
iC_7	0.6	0.5	0.5	0.3	0.4	0.2	0.5	0.5
nC_7	0.8	0.7	1.0	0.5	0.4	0.4	0.6	0.4
ECP + MCH	0.9	0.7	0.9	0.7	0.6	0.9	0.5	1.0
Tol	4.8	5.2	4.2	4.2	1.4	1.8	1.6	2.2
iC_8	23.9	52.5	23.5	41.7	32.6	46.7	31.4	46.1
PCP + ECH	1.7	0.6	1.1	0.8	0.5	1.2	0.5	1.0
EtBz	11.8	3.4	12.0	6.6	6.8	5.9	7.1	5.9
*p*Xyl	4.7	1.2	5.3	2.6	4.9	2.5	4.7	2.7
*m*Xyl	13.4	5.5	14.3	8.7	13.5	8.7	14.2	8.9
*o*Xyl	11.6	3.8	16.6	13.8	18.5	15.5	18.8	16.3
iC_9	4.1	4.0	3.0	3.1	3.6	2.7	3.1	2.2
nC_9	0	0.2	0	0.1	0.1	0.2	0	0
Coke (%)	–	0.53	–	0.49	–	0.42	–	0.41

TOS $T = 450$ °C; $P = 1$ MPa; WHSV = 3.4; H_2/nC_8(molar) = 7.3. Coke deposited after 360 min TOS.

formation of *o*-xylene, an important petrochemical feedstock to produce maleic anhydride.

4. Conclusions

Both rhenium and germanium affect the electronic properties of Pt in $Pt–Re–Ge/Al_2O_3$. The three elements partly form alloys among them which are inactive for CH dehydrogenation. The dehydrogenation activity is due to Pt interacted with the other elements, $Pt^{\delta+}$ or $Pt^{\delta-}$, that are less active than Pt^0. The addition of germanium to both monometallic and bimetallic platinum-based catalyst increases the isomerization activity and reduces aromatization and hydrogenolysis. The addition of both rhenium and germanium increases the formation of *o*-xylene, an important petrochemical feedstock. The trimetallic was the most active and stable catalyst during the *n*-octane reaction and showed selectivities to aromatics and isomers very similar to the one of the germanium bimetallic catalyst.

Acknowledgments

Authors acknowledge the financial assistance of CONICET, UNL, CAPES/SCyT, FINEP and CNPq.

References

[1] B.C. Gates, J.R. Katzer and G.C.A. Schuit, *Chemistry of Catalytic Processes* (McGraw Hill Book Comp., New York, 1979).
[2] M.D. Adgar, in: *Applied Industrial Catalysis*, Vol. 1, ed. E. Leach (Academic Press, New York), p. 124.
[3] C.N. Satterfield, *Processing of Petroleum and Hydrocarbons in Heterogeneous Catalysis in Practice* (McGraw Hill Book Comp, New York, 1980).
[4] J.M. Parera and N.S. Fígoli, in: *Catalytic Naphtha Reforming*, eds. G.J. Antos, A.M. Aitani and J.M. Parera (Marcel Dekker, Inc., New York, 1995), p. 45.
[5] J.M. Parera and J.N. Beltramini, J. Catal. 112 (1988) 357.
[6] F.H. Ribeiro, A.L. Bonivardi, C. Kim and G.A. Somorjai, J. Catal. 150 (1994) 186.
[7] N. Wagstaff and R. Prins, J. Catal. 59 (1979) 434.
[8] G.B. Mc Vicker, R.L. Garte and R.T.K. Baker, J. Catal. 54 (1978) 129.
[9] V.K. Shum, J.B. Butt and W.M.H. Schatler, J. Catal. 99 (1986) 126.
[10] R.L. Meiville, J Catal. 87 (1984) 437.
[11] C.L. Pieck, P. Marecot and J. Barbier, Appl. Catal. A 143 (1996) 283.
[12] L.S. Carvalho, C.L. Pieck, M.C. Rangel, N.S. Fígoli, J.M. Grau, P. Reyes and J.M. Parera, Appl. Catal. A 269 (2004) 91.
[13] L.S. Carvalho, C.L. Pieck, M.C. Rangel, N.S. Fígoli, C.R. Vera and J.M. Parera, Appl. Catal. A 269 (2004) 105.
[14] G.J. Antos, U.S. Pat. 4,312,788, to UOP, 1982.
[15] C.D. Wagner, L.E. Davis, M.V. Zeller, J.A. Taylor, R.H. Raymond and L.H. Gale, Surf. Interf. Anal. 3 (1981) 211.
[16] H. Lieske, G. Lietz, H. Spindler and J. Volter, J. Catal. 81 (1983) 8.

[17] S.R. de Miguel, O.A. Scelza and A.A. Castro, Appl. Catal. 44 (1988) 23.
[18] S.R. de Miguel, J.M. Parera, G.T. Baronetti, A.A. Castro and O.A. Scelza, Appl. Catal. 60 (1990) 47.
[19] J. Goldwasser, B. Arenas, J. Bolívar, G. Castro, A. Rodríguez, A. Fleitas and J. Giron, J. Catal. 100 (1986) 75.
[20] R. Bouwman and P. Biloen, J. Catal. 48 (1997) 200.
[21] J.H. Sinfelt, *Bimetallic Catalysts* (John Willey & Sons, New York, 1983).
[22] J.P. Botiaux, J.M. Devés, B. Didillon and C.R. Marcilly, in: *Catalytic Naphtha Reforming*, eds. G.J. Antos, A.M. Aitani and J.M. Parera (Marcel Dekker, Inc., New York, 1995), p. 79.
[23] D.R. Ardiles, S.R. de Miguel, A.A. Castro and O.A. Scelza, Appl. Catal. 24 (1986) 175.
[24] M.G.V. Mordente and C.H. Rochester, J. Chem. Soc. Far. Trans. I 85 (1989) 3405.
[25] F.C. Galisteo, R. Mariscal, J.L.G. Fierro, G. Collins, J.C. Yori and J.M. Parera, XIX Iberoam. Symp. Catal., Mexico, 2004, p. 3205.
[26] A.V. Ivanov, A. Yu Stakheev and L.M. Kustov, Russ. Chem. Bull. 47 (1999) 1255.
[27] J. Volter, H. Lieske and G. Lietz, React. Kin. Catal. Lett. 16 (1981) 87.
[28] N. Macleod, J.R. Fryer, D. Stirling and G. Bebb, Catal. Today 46 (1998) 37.
[29] G.A. Mills, H. Heinemann, T.H. Milliken and A.G. Oblad, Ind. Eng. Chem. 45 (1953) 134.
[30] C.A. Querini, N.S. Fígoli and J.M. Parera, Appl. Catal. 52 (1989) 249.